Journal of Power Sources 189 (2009) 28–33

Contents lists available at ScienceDirect

Journal of Power Sources

journal homepage: www.elsevier.com/locate/jpowsour

Synthesis and characterization of $LiNi_{0.6}Mn_{0.4-x}Co_xO_2$ as cathode materials for Li-ion batteries

Jiangang Li [a], Li Wang [b], Qian Zhang [a], Xiangming He [a,b,*]

[a] School of Chemical Engineering, Beijing Institute of Petrochemical Technology, Beijing 102617, PR China
[b] Insitute of Nuclear & New Energy Technology, Tsinghua University, Beijing 100084, PR China

ARTICLE INFO

Article history:
Received 1 July 2008
Received in revised form
21 November 2008
Accepted 11 December 2008
Available online 24 December 2008

Keywords:
Cathode materials
Layered composite oxide
$LiNi_{0.6}Mn_{0.4-x}Co_xO_2$
Li-ion battery

ABSTRACT

$LiNi_{0.6}Co_xMn_{0.4-x}O_2$ (x = 0.05, 0.10, 0.15, 0.2) cathode materials are prepared, and their structural and electrochemical properties are investigated using X-ray diffraction (XRD), scanning electron microscope (SEM), X-ray photoelectron spectroscopy (XPS), differential scanning calorimetric (DSC) and charge–discharge test. The results show that well-ordering layered $LiNi_{0.6}Co_xMn_{0.4-x}O_2$ (x = 0.05, 0.10, 0.15, 0.2) cathode materials are successfully prepared in air at 850 °C. The increase of the Co content in $LiNi_{0.6}Mn_{0.4-x}Co_xO_2$ leads to the acceleration of the grain growth, the increase of the initial discharge capacity and the deterioration of the cycling performance of $LiNi_{0.6}Mn_{0.4-x}Co_xO_2$. It also leads to the enhancement of the ratio Ni^{3+}/Ni^{2+} in $LiNi_{0.6}Co_xMn_{0.4-x}O_2$, which is approved by the XPS analysis, resulting in the increase of the phase transition during cycling. This is speculated to be main reason for the deteriotion of the cycling performance. All synthesized $LiNi_{0.6}Co_xMn_{0.4-x}O_2$ samples charged at 4.3 V show exothermic peaks with an onset temperature of larger than 255 °C, and give out less than 400 J g^{-1} of total heat flow associated with the peaks in DSC analysis profile, exhibiting better thermal stability. $LiNi_{0.6}Co_{0.05}Mn_{0.35}O_2$ with low Co content and good thermal stability presents a capacity of 156.6 mAh g^{-1} and 98.5% of initial capacity retention after 50 cycles, showing to be a promising cathode materials for Li-ion batteries.

1. Introduction

$LiCoO_2$ has been widely used as cathode material for lithium-ion batteries due to its high capacity and excellent cycling stability. Nonetheless, cobalt has economic and environmental problems that leave the door open to exploit alternative cathode materials, such as layered $LiNiO_2$ [1,2], $LiMnO_2$ [3,4], spinel $LiMn_2O_4$ [5,6]. Unfortunately, these materials still have significant drawbacks. The major problems associated with $LiNiO_2$ include the difficult to prepare a stoichiometric $LiNiO_2$ powders without cation mixing, the structure degradation caused by irreversible phase transition during electrochemical cycling [7,8], thermal safety problems caused by oxygen release in the charged state. The main shortcoming of layered $LiMnO_2$ is the crystallographic transformation to spinel structure during electrochemical cycling [3,4,9]. $LiMn_2O_4$ presents smaller capacity, and significant capacity fading during cycling at elevated temperature due to several probabilities, e.g., manganese dissolution, electrolyte decomposition, Jahn-Teller distortion [10,11]. Various approaches such as partial replacement of nickel and manganese by transition metals, surface coating, optimizing preparation methods and conditions were adopted to improve their performance [6,12–15].

The most appropriate and successful approach is to introduce Ni, Co and Mn ions simultaneously in the layer structure. A solution of $LiNi_{1-x-y}Co_xMn_yO_2$ may possess improved performances, such as thermal stability, due to the co-operation effect of the three ions. Recently, intensive effort has been directed towards development of $LiNi_xCo_{1-2x}Mn_xO_2$ as possible replacement for $LiCoO_2$ [16–23]. Now $LiNi_{1/3}Co_{1/3}Mn_{1/3}O_2$ and $LiNi_{0.4}Co_{0.2}Mn_{0.4}O_2$ have been commercialized and used widely in commercial lithium-ion batteries due to lower cost, better electrochemical performance and thermal stability. However, these materials show low capacities of only ~150 mAh g^{-1}.

Lithium nickel cobalt manganese composite oxide with higher capacity can be obtained while the nickel content increases in such material. Investigation of the preparation and the electrochemical properties of $LiNi_{1-x-y}Co_xMn_yO_2$ ($0 \le x \le 0.5$, $0 \le y \le 0.3$) show that $LiNi_{0.7}Co_{0.2}Mn_{0.1}O_2$ is a material of high capacity and good cycleability. The excess Mn doping in case of $LiNi_{0.5}Co_{0.2}Mn_{0.3}O_2$ returns a cycle life as poor as that of pristine $LiNiO_2$ [24]. Yoshio et al. [25] have studied the preparation and properties of $LiNi_{0.8-y}Co_yMn_{0.2}O_2$ ($0 \le y \le 0.3$), and successfully

* Corresponding author at: Insitute of Nuclear & New Energy Technology, Tsinghua University, Beijing 100084, PR China. Tel.: +86 10 89796073; fax: +86 10 89796031.
E-mail address: hexiangming@tsinghua.org.cn (X. He).

0378-7753/$ – see front matter © 2008 Elsevier B.V. All rights reserved.
doi:10.1016/j.jpowsour.2008.12.046

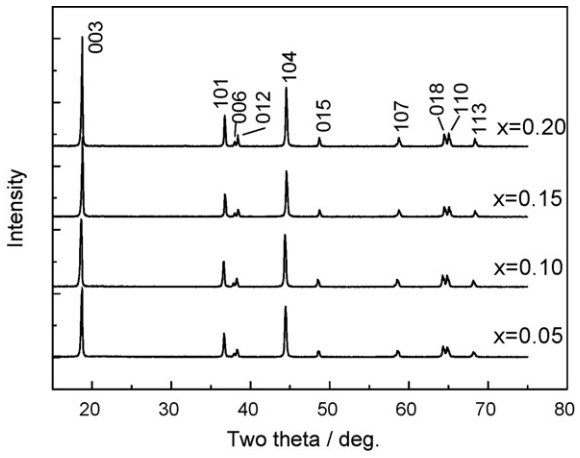

Fig. 1. XRD patterns of $LiNi_{0.6}Mn_{0.4-x}Co_xO_2$.

synthesized $LiNi_{0.8-y}Co_yMn_{0.2}O_2$ with discharge capacities greater than 155 mAh g^{-1} in air. Chen et al. [26] has prepared single-phase electroactive $LiNi_{0.8-x}Co_xMn_{0.2}O_2$ ($x = 0.05$, 0.10, 0.20) compounds by heating the precursor $Ni_{0.8-x}Co_xMn_{0.2}(OH)_2$ and Li_2CO_3 in air at 850–900 °C. $LiNi_{0.7}Co_{0.1}Mn_{0.2}O_2$ and $LiNi_{0.6}Co_{0.2}Mn_{0.2}O_2$ with an initial discharge capacities of 150 mAh g^{-1} have been reported to have the best electrochemical characteristics among the three materials. Liao et al. [27] have synthesized $LiNi_{0.6}Co_{0.4-x}Mn_xO_2$ ($x = 0.15$, 0.2, 0.25) materials in O_2 by the mixing hydroxide method. $LiNi_{0.6}Co_{0.25}Mn_{0.15}O_2$ calcined at 900 °C exhibits the good electrochemical characteristics, showing the initial discharge capacity of 178.4 mAh g^{-1} and the capacity retention of 98.1% after 20 cycles. Kim et al. [14] has reported that $Li[Ni_{0.8}Co_{0.2-x}Mn_x]O_2$ ($x = 0$, 0.1) prepared in O_2 atmosphere can deliver a discharge capacity of 197–202 mAh g^{-1} and shows good cycling performance. Compared to $Li[Ni_{0.8}Co_{0.2}]O_2$, $Li[Ni_{0.8}Co_{0.1}Mn_{0.1}]O_2$ exhibits better thermal stability because of the improvement of structural stability due to Mn substitution. The properties of $LiNi_{0.6}Co_{0.2}Mn_{0.2}O_2$ prepared by a carbonate co-precipitation method [28], hydroxide co-precipitation method [29] and solid-state reaction [30] have also been investigated. The material prepared at 850–900 °C in air or O_2 exhibits an electrochemical properties of initial capacity of about 170 mAh g^{-1} and better cycleability.

Table 1
Lattice parameters of $LiNi_{0.6}Mn_{0.4-x}Co_xO_2$ samples.

Sample		a (Å)	c (Å)	c/a	I_{003}/I_{104}
$LiNi_{0.6}Co_xMn_{0.4-x}O_2$	$x = 0.05$	2.8727	14.2306	4.954	1.358
	$x = 0.10$	2.8744	14.2600	4.961	1.291
	$x = 0.15$	2.8647	14.1917	4.954	1.732
	$x = 0.20$	2.8661	14.1978	4.954	1.849

Although $LiNi_{1-x-y}Co_xMn_yO_2$ with higher capacity have been studied by some groups, less attention has been paid on the preparation and properties of $LiNi_{1-x-y}Co_xMn_yO_2$ with Mn content $0.2 \le y \le 0.4$ and Co content $0 \le x \le 0.2$. In this study, $LiNi_{0.6}Mn_{0.4-x}Co_xO_2$ ($x = 0.05$, 0.1, 0.15, 0.2) were synthesized in air. The structural properties, morphology, electrochemical properties and thermal stability of $LiNi_{0.6}Mn_{0.4-x}Co_xO_2$ powders were investigated.

2. Experimental

$LiNi_{0.6}Mn_{0.4-x}Co_xO_2$ were prepared by mixing homogenous $Ni_{0.6}Mn_{0.4-x}Co_x(OH)_2$ precursor with 5% excess $LiOH{\cdot}H_2O$ thoroughly and heating at 850 °C for 20 h in air. The heating temperature was chosen after experiments for heating temperature optimization.

Powder X-ray diffraction (SHIMADZU, XRD7000) measurements using Cu Kα radiation were used to characterize the structures of the powders. Particle morphology of the powders was observed

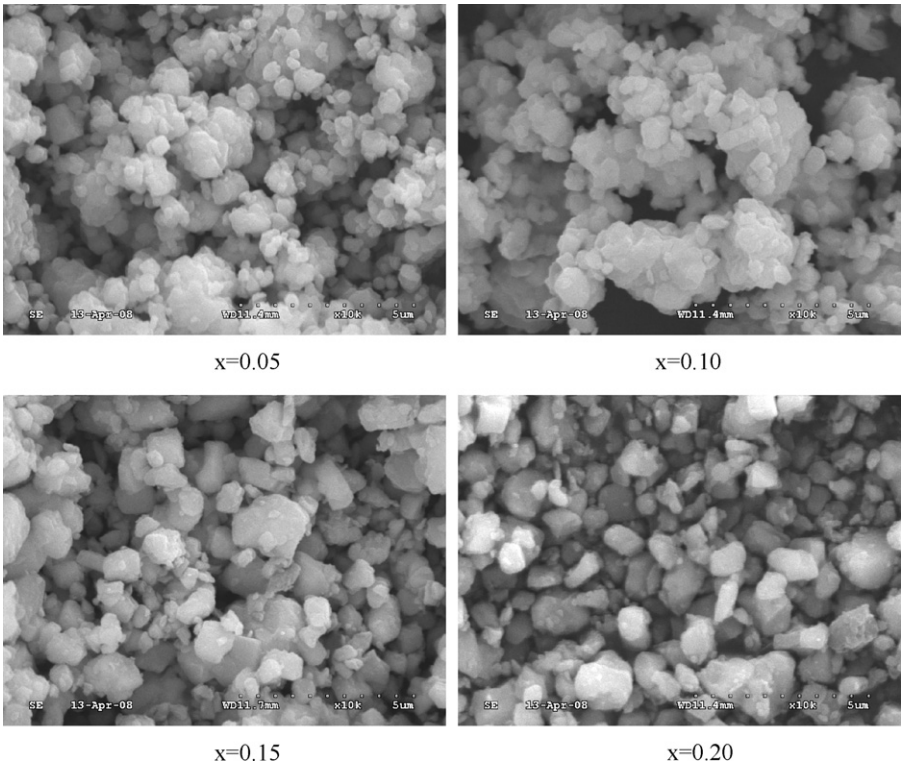

Fig. 2. SEM images of $LiNi_{0.6}Mn_{0.4-x}Co_xO_2$.

using a scanning electron microscope (SEM, HITCHI S-3500). X-ray photoelectron spectroscopy (XPS, PHI-5800) measurements were conducted to determine the oxidation states of Ni and Mn. Al Kα (1486 eV) radiation was the primary excitation source, and the energy scale was adjusted based on the carbon peak in the C^{1s} spectra at 284.6 eV.

The electrochemical characterization was performed using CR2032 coin-type cells. The cell consisted of a cathode with the composition of 88 wt.% $LiNi_{0.6}Mn_{0.4-x}Co_xO_2$, 6 wt. % carbon black, and 6 wt.% PVDF, a lithium metal anode separated by a Celguard 2400 microporous film. The electrolyte was 1 M $LiPF_6$ EC + DEC + DMC (1:1:1 by volume). The cell was assembled in argon-filled dry box. The charge–discharge tests were galvanostatically performed over 2.5–4.3 V at 30 mA g^{-1}. For the differential scanning calorimetric (DSC) experiments, after the coin cells were galvanostatically charged and discharged three cycles at 30 mA g^{-1}, the cells were then fully charged to 4.3 V and opened in argon-filled dry box. The extra electrolyte was removed from the surface of the electrode, and the electrode materials were collected from the current collector, and then used for DSC measurements. The measurements were carried out in a Pekin-Elemer Pyris 1 DSC at a scan rate of 1 °C min^{-1}.

3. Results and discussion

Fig. 1 displays the X-ray diffraction patterns of $LiNi_{0.6}Mn_{0.4-x}Co_xO_2$ (x = 0.05, 0.10, 0.15, 0.2) prepared in air, respectively. All diffraction peaks in each of the patterns are indexed on the basis of the α-$NaFeO_2$ structure ($R3m$). Unit cell parameters are calculated and summarized in Table 1. The clear splitting of the lines assigned to the Miller indices (0 0 6,1 0 2) and (1 0 8,1 1 0) in Fig. 1, and the ratio I_{003}/I_{104} of greater than 1.2 listed in Table 1, show that all synthesized powders presents well-ordering layered α-$NaFeO_2$ structure. The results also indicate that well-ordering layered $LiNi_{0.6}Co_xMn_{0.4-x}O_2$ (x = 0.05, 0.10, 0.15, 0.2) can be prepared in air at 850 °C.

Fig. 2 shows the SEM images of $LiNi_{0.6}Mn_{0.4-x}Co_xO_2$ (x = 0.05, 0.10, 0.15, 0.2) samples. The particles of sample with x value of 0.05 are formed by agglomeration of many small crystal particles with

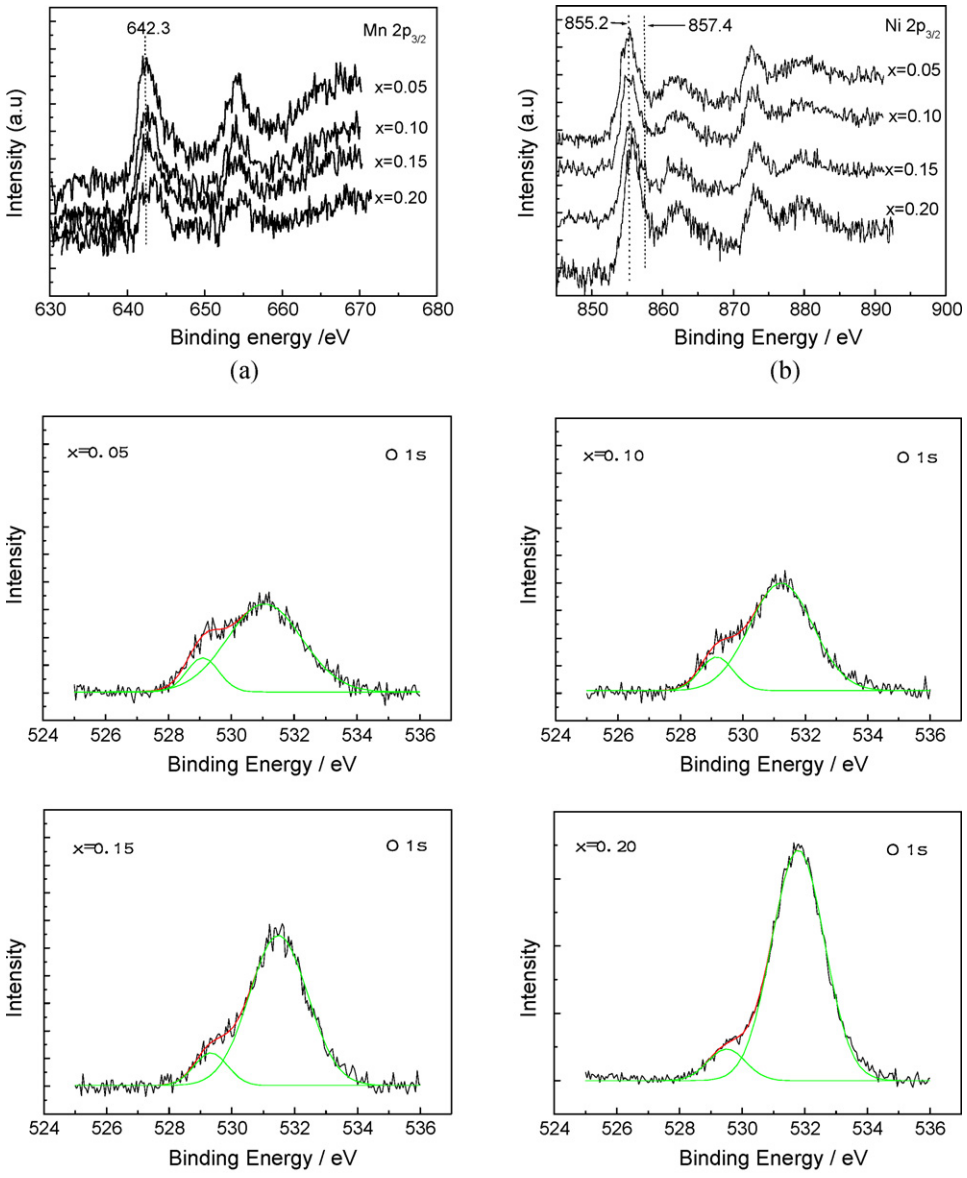

Fig. 3. XPS spectra of (a) Mn $2p_{3/2}$, (b) Ni $2p_{3/2}$, and (c) O 1s for $LiNi_{0.6}Mn_{0.4-x}Co_xO_2$.

size of about 200–500 nm. With the increase of the Co content (x value to 0.20), the agglomerated small crystal particles are sintered together to form larger grain particles with size of about 0.5–2 μm. Co doping accelerates the grain growth of $LiNi_{0.6}Mn_{0.4-x}Co_xO_2$, which can improve the tap density.

Fig. 3 shows the XPS spectra of Mn $2p_{3/2}$, Ni $2p_{3/2}$, and O 1s for $LiNi_{0.6}Mn_{0.4-x}Co_xO_2$. The O 1s peak at about 529 eV corresponds to the lattice oxygen [31]. The binding energy is shown to be 529.1, 529.2, 529.3, 529.5 eV for Co content x value 0.05, 0.10, 0.15, 0.20 in $LiNi_{0.6}Mn_{0.4-x}Co_xO_2$ sample, respectively. The binding energy of O 1s shifts slightly to higher value with the increase of Co content, which is similar to that reported by Sun et al. [18]. It can be ascribed to stronger Co–O than Mn–O. Another O 1s peak at about 531 eV corresponds to the absorbed oxygen, which come from surface CO_3^{2-} and –OH, a common impurity at the surface of air exposed $LiMO_2$ materials, resulting from the adsorption of CO_2 and water from the ambient either upon storage or during synthesis process [31]. The ration S_a/S_l of O 1s peak area for absorbed oxygen S_a to lattic oxygen S_l is shown to be 6.0, 6.1, 8.1, 10.2 for Co content x value 0.05, 0.10, 0.15, 0.20 in $LiNi_{0.6}Mn_{0.4-x}Co_xO_2$ sample, respectively. That indicates that the amount of surface CO_3^{2-} and –OH impurity also increases with the increase of the Co content. Moreover, the Mn $2p_{3/2}$ spectra of the samples with different amounts of cobalt are very similar. For $x = 0.05$, the Mn $2p_{3/2}$ peak is observed at 642.3 eV, demonstrating the good correlation with the value (642.1 eV) reported by Kang et al. [32] and the value (642.4 eV) for $LiNi_{0.33}Co_{0.33}Mn_{0.33}O_2$, the value (642.5 eV) for $LiNi_{0.6}Co_{0.2}Mn_{0.2}O_2$ reported by Kosova et al. [33]. With the increase of the Co content x, the Mn $2p_{3/2}$ peak is shifted slightly to 643.0 eV, even though both values are rather typical for Mn^{4+} oxides. The peak shifting to higher binding energy with the increase of Co addition has been ascribed by Sun et al. [18] to the electronic structure of Mn ions affected by addition of Co. The Ni $2p_{3/2}$ peak for $x = 0.05$ is observed at 855.2 eV. That is higher than that reported by Kang et al. (854.3 eV) [32], which can be attributed to the presence of Ni in both 2+ and 3+ valence state. With the increase of the Co content, the center of Ni $2p_{3/2}$ peak shifts to higher values, and a shoulder peak at 857.4 eV, being same as the Ni $2p_{3/2}$ peak value of Ni_2O_3 reported in literature [18], becomes obvious and stronger. This indicates that the ratio of Ni^{3+}/Ni^{2+} in $LiNi_{0.6}Mn_{0.4-x}Co_xO_2$ become greater while the Co content increases. It can be concluded that the oxidation state of Mn is maintained at 4+ regardless of Co content and the charge compensation mechanism concerns mostly the Ni oxidation states.

Fig. 4 shows the first charge–discharge curves for the synthesized $LiNi_{0.6}Mn_{0.4-x}Co_xO_2$ electrodes over 2.5–4.3 V. The discharge capacity is shown to be 156.9, 164.2, 166.8, 172.8 mAh g^{-1} for Co content x value 0.05, 0.10, 0.15, 0.20 in $LiNi_{0.6}Mn_{0.4-x}Co_xO_2$ sample, respectively. The discharge capacity is improved as Co content in $LiNi_{0.6}Mn_{0.4-x}Co_xO_2$ increases. This is in agreement with the results of $LiNi_{0.6}Mn_{0.4-x}Co_xO_2$ ($x = 0.15, 0.20, 0.25$) reported by Liao et al. [27]. Because the increase in discharge capacity is consistent with the increase of ratio $I_{(003)}/I_{(104)}$, which has been reported to be closely related to the undesirable cation mixing [34], the decrease of cation disordering with the increase of Co content in $LiNi_{0.6}Mn_{0.4-x}Co_xO_2$ leads to the improvement of capacity. The capacity of sample with $x = 0.20$ is very similar to that reported in literature [27,28]. This reassures that $LiNi_{0.6}Co_xMn_{0.4-x}O_2$ ($x = 0.05$, 0.10, 0.15, 0.2) with better electrochemical active can be prepared in air at 850 °C.

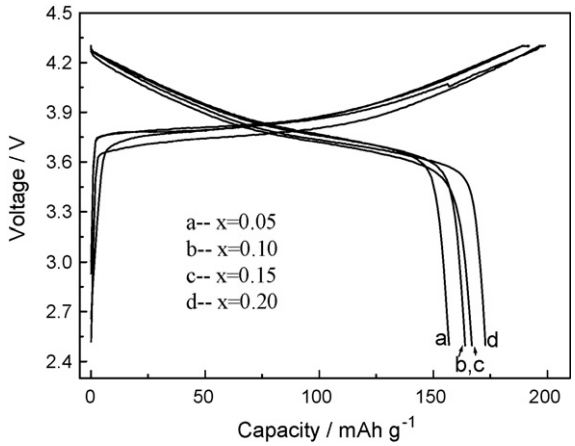

Fig. 4. First charge–discharge curves of $LiNi_{0.6}Co_xMn_{0.4-x}O_2$.

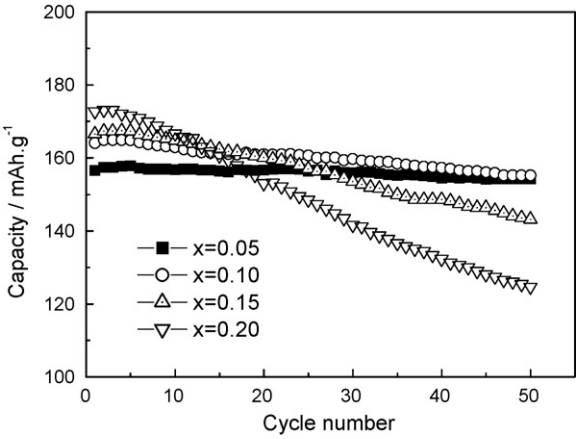

Fig. 5. Cycling performance of $LiNi_{0.6}Mn_{0.4-x}Co_xO_2$.

Although the initial discharge capacity is improved with the increase of the Co content, the cycleability of $LiNi_{0.6}Mn_{0.4-x}Co_xO_2$ is deteriorated, as shown in Fig. 5. When charge–discharged over 2.5–4.3 V for 50 cycles, the sample with $x = 0.20$ shows fast capacity fading, and only 71.5% of its initial capacity remains. However, when Co content x decreases to 0.05, the sample shows a capacity of 156.6 mAh g^{-1}, and 98.5% of initial capacity retention after 50 cycles, exhibiting the best electrochemical performance among the four samples.

What is the reason for the deterioration of cycleability of $LiNi_{0.6}Mn_{0.4-x}Co_xO_2$ with the increase of the Co content? One main reason for the capacity fading of $LiMO_2$ (M = Ni, Co, Mn) is structural change during charge/discharge cycling, for example, irreversible change from layered phase to spinel phase for $LiMnO_2$ [35,36], and characteristic reversible structure change in charge/discharge process for $LiNi_{1-x}Co_xO_2$ [37,38]. Although the structure change in charge/discharge process for $LiNi_{1-x}Co_xO_2$ is reversible, more phase change has been proved to deteriorate the cycling capacity stability. The reason has been unclear up to now. We think it may be attributed to the impedance increase of $LiNi_{1-x}Co_xO_2$ electrode come from faster pulverization of $LiNi_{1-x}Co_xO_2$ crystal particles and poorer particles contact with conducting additive carbon black. The reduction of the phase transition in charge/discharge process, e.g. $LiNi_{1-x}Co_xO_2$ by Mn doping [14] and Al doping [39], can improve the cycling stability. Fig. 6 shows the differential capacity curves of $LiNi_{0.6}Co_xMn_{0.4-x}O_2$ during second cycle. Broadened anodic peaks at 3.80 V as well as cathodic peaks at 3.77 V can be observed for $x = 0.05$, showing single phase reaction in charge/discharge process. However, anodic peaks at 3.73 and 3.78 V for $x = 0.10$, anodic peaks at 3.71 and 3.78 V for $x = 0.15$, as well as anodic peaks at 3.67 and 3.78 V for $x = 0.20$ are observed, indicating that the phase transition in the charge/discharge process are strongly accelerated with the increase of Co content in $LiNi_{0.6}Co_xMn_{0.4-x}O_2$. The acceleration on the phase transition should be attributed to the increase of Ni^{3+} content in $LiNi_{0.6}Co_xMn_{0.4-x}O_2$. Because Mn ion

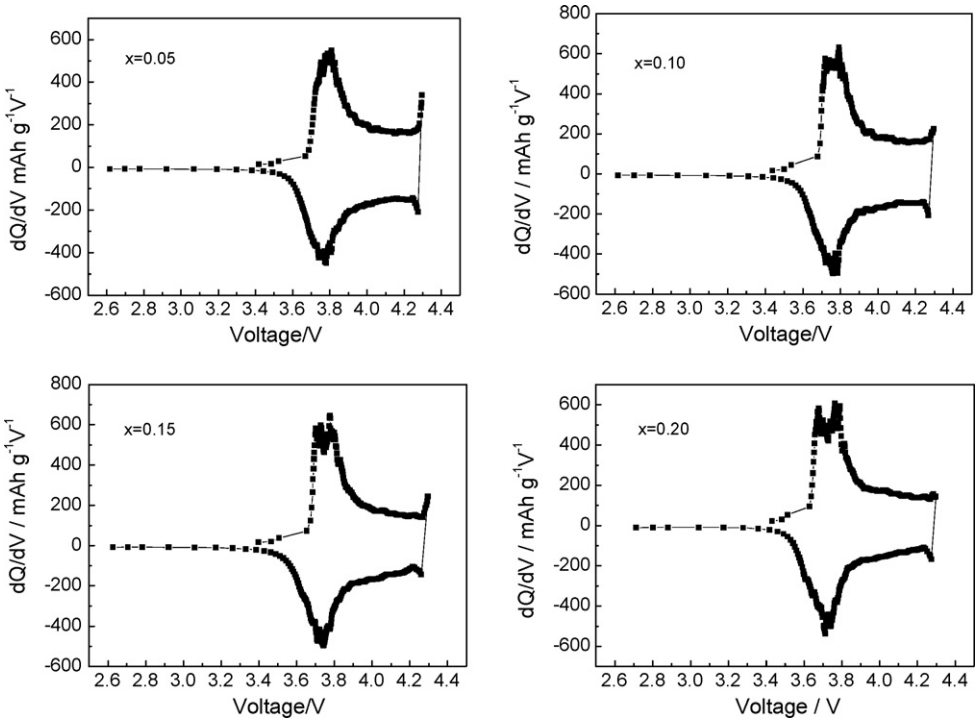

Fig. 6. Differential capacity vs. voltage curves of $LiNi_{0.6}Co_xMn_{0.4-x}O_2$ during second cycle.

with the oxidation state of 4+ is inactive over the voltage rang of 2.5–4.3 V, the charge/discharge reaction should correspond to both Ni^{2+}/Ni^{4+} and Ni^{3+}/Ni^{4+} redox couple. Ni^{2+}/Ni^{4+} redox couple in $LiNi_xCo_{1-2x}Mn_xO_2$ corresponds to a single phase reaction [16–23], but Ni^{3+}/Ni^{4+} redox couple in $LiNi_{1-x}Co_xO_2$ corresponds to more phase transition reaction in charge/discharge process [1,37,38,40]. The increase of the Co content leads to the increase of the ratio Ni^{3+}/Ni^{2+} in $LiNi_{0.6}Co_xMn_{0.4-x}O_2$, as approved by the XPS analysis, which can increase the phase transition in charge/discharge process and may cause the deterioration of the cycling performance.

Fig. 7 shows DSC profiles of $LiNi_{0.6}Co_xMn_{0.4-x}O_2$ charged to 4.3 V. The sample with $x = 0.05$ shows two distinct exothermic peaks with an onset temperature of 255.7 °C and 398.3 J g^{-1} of total heat associated with the two peaks. The DSC curves of sample with $x = 0.10$ is similar to that of $x = 0.05$, but the total heat associated with the two peaks is 283.0 J g^{-1}. The sample with $x = 0.15$ exhibits one sharp exothermic peak at 282.5 °C with an onset temperature of 259.1 °C and 397.2 J g^{-1} of heat associated with the exothermic peak. The sample with $x = 0.20$ show higher onset temperature (259.8 °C) and exothermic peak temperature (286.3 °C), but much smaller amount of heat (223.1 J g^{-1}) than the other materials. Consequently, the sample with $x = 0.20$ have better thermal safety characteristics than the other three samples. These data are very similar to that of $LiNi_{3/8}Co_{2/8}Mn_{3/8}O_2$, and much smaller than that of $LiNiO_2$ and $LiCoO_2$ [16], indicating that all synthesized $LiNi_{0.6}Co_xMn_{0.4-x}O_2$ samples present better thermal stability.

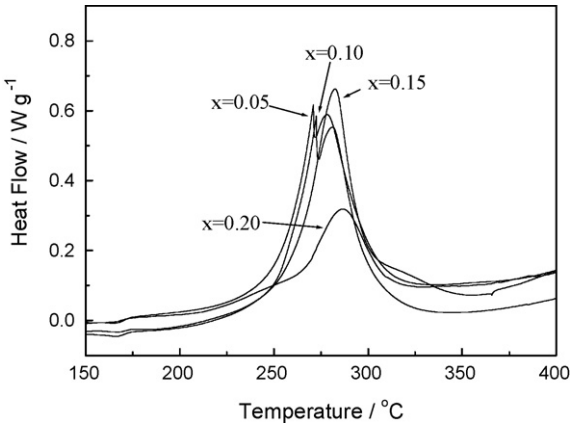

Fig. 7. DSC profiles of $LiNi_{0.6}Mn_{0.4-x}Co_xO_2$ at 4.3 V.

4. Conclusion

Well-ordering layered $LiNi_{0.6}Co_xMn_{0.4-x}O_2$ ($x = 0.05$, 0.10, 0.15, 0.2) cathode materials can be successfully prepared in air at 850 °C in this study. The increase of Co content in $LiNi_{0.6}Mn_{0.4-x}Co_xO_2$ leads to the acceleration of the grain growth and the improvement of the initial discharge capacity, but the deterioration of the cycleability. The XPS analysis shows that the increase of the Co content can lead to the enhancement of the ratio Ni^{3+}/Ni^{2+} in $LiNi_{0.6}Co_xMn_{0.4-x}O_2$, further leading to the increase of the phase transition in charge/discharge process, finally resulting in the deterioration of the cycling performance. DSC analysis indicates that all synthesized $LiNi_{0.6}Co_xMn_{0.4-x}O_2$ samples exhibit good thermal stability. This study demonstrates that $LiNi_{0.6}Co_{0.05}Mn_{0.35}O_2$ is a promising cathode material for Li-ion batteries.

Acknowledgements

The financial supports from the Scientific Research Common Program of Beijing Municipal Commission of Education (KM200710017001) and Funding Project for Academic Human Resources Development in Institutions of Higher Learning under the Jurisdiction of Beijing Municipality are highly appreciated. The authors also highly appreciate the revision comments from the anonymous reviewers.

References

[1] C. Delmas, M. Menetrier, L. Croguennec, I. Saadoune, A. Rougier, C. Pouillerie, G. Prado, M. Grune, L. Fournes, Electrochim. Acta 45 (1999) 243.

[2] M.E. Spahr, P. Novak, B. Schnyder, J. Electrochem. Soc. 145 (1998) 1113.
[3] I. Koetschau, M.N. Richard, J.R. Dahn, J. Electrochem. Soc. 142 (1995) 2906.
[4] R.J. Gummov, M.M. Thackery, J. Electrochem. Soc. 141 (1994) 1178.
[5] J.M. Tarascon, E. Wang, F.K. Shokoohi, W.R. Mckinnon, S. Colson, J. Electrochem. Soc. 138 (1991) 2859.
[6] A.D. Robertson, S.H. Lu, W.F. Averill, J. Howard, J. Electrochem. Soc. 144 (1997) 3500.
[7] R. Stoyanov, E. Zhecheva, R. Alca′ntara, Solid State Ionics 161 (2003) 197.
[8] D.D. Macneil, Z.H. Lu, J.R. Dahn, J. Power Sources 108 (2002) 8.
[9] F. Capitaine, P. Gravereau, C. Delmas, Solid State Ionics 89 (1996) 197.
[10] Y.-Y. Xia, Y.-H. Zhou, M.J. Yoshio, J. Electrochem. Soc. 144 (1997) 2593.
[11] J.M. Tarascon, W.R. Mckinnon, F. Coowar, T.N. Bowmer, G. Amatucci, D. Guyomard, J. Electrochem. Soc. 141 (1994) 1421.
[12] Z.-P. Guo, G.-X. Wang, H.-K. Liu, S.-X. Dou, Solid State Ionics 148 (2002) 359.
[13] J.-G. Li, X.-M. He, R.-S. Zhao, Trans. Nonferrous Met. Soc. China 17 (2007) 1324.
[14] M.-H. Kim, H.-S. Shin, D. Shin, Y.-K. Sun, J. Power Sources 159 (2006) 1328.
[15] S.B. Majumder, S. Nieto, R.S. Katiyar, J. Power Sources 154 (2006) 262–267.
[16] Z. Lu, D.D. MacNeil, J.R. Dahn, Electrochem. Solid-State Lett. 4 (2001) A200.
[17] I. Belharouak, Y.-K. Sun, J. Liu, K. Amine, J. Power Sources 123 (2003) 247.
[18] Y. Sun, C. Ouyang, Z. Wang, X. Huang, L. Chen, J. Electrochem. Soc. 151 (2004) A504.
[19] D.-Ch. Li, H. Noguchi, M. Yoshio, Electrochim. Acta 50 (2004) 427.
[20] P. He, H. Wang, L. Qi, T. Osaka, J. Power Sources 160 (2006) 627.
[21] J. Choi, A. Manthiram, Solid State Ionics 176 (2005) 2251.
[22] M. Ma, N.A. Chernova, B.H. Toby, P.Y. Zavalij, M.S. Whittingham, J. Power Sources 165 (2007) 517.
[23] L. Zhang, X. Wang, T. Muta, D. Li, H. Noguchi, M. Yoshio, R. Ma, K. Takada, T. Sasaki, J. Power Sources 162 (2006) 629.
[24] Z. Liu, A. Yu, J.Y. Lee, J. Power Sources 81/82 (1999) 416.
[25] M. Yoshio, H. Noguchi, J. Itoh, M. Okada, T. Mouri, J. Power Sources 90 (2000) 176.
[26] Y. Chen, G.X. Wang, K. Konstantinov, H.K. Liu, S.X. Dou, J. Power Sources 119–121 (2003) 184.
[27] P.Y. Liao, J.G. Duh, S.R. Sheen, J. Power Sources 143 (2005) 212.
[28] Y. Zhang, H. Cao, J. Zhang, B. Xia, Solid State Ionics 177 (2006) 3303.
[29] H. Cao, Y. Zhang, J. Zhang, B. Xia, Solid State Ionics 176 (2005) 1207.
[30] C. Gan, X. Hu, H. Zhan, Y. Zhou, Solid State Ionics 176 (2005) 687.
[31] A.W. Moses, H.G. Garcia Flores, J.-G. Kim, M.A. Langell, Appl. Surf. Sci. 253 (2007) 4782.
[32] S.-H. Kang, J. Kim, M.E. Stoll, D. Abraham, Y.K. Sun, K. Amine, J. Power Sources 112 (2002) 41.
[33] N.V. Kosova, E.T. Devyatkina, V.V. Kaichev, J. Power Sources 174 (2007) 965–969.
[34] C. Delmas, I. Saadoune, A. Rougier, J. Power Sources 89 (1996) 43.
[35] G. Vitins, K. West, J. Electrochem. Soc. 144 (1997) 2587.
[36] Y.I. Jang, B. Huang, Y.-M. Chiang, D.R. Sadoway, Electrochem. Solid-State Lett. 1 (1998) 13.
[37] W. Li, J.N. Reimers, J.R. Dahn, Solid State Ionics 67 (1993) 123.
[38] G.X. Wang, M.J. Lindsay, M. Ionescu, D.H. Bradhurst, S.X. Dou, H.K. Liu, J. Power Sources 97/98 (2001) 298.
[39] S.B. Majumder, S. Nieto, R.S. Katiyar, J. Power Sources 154 (2006) 262.
[40] E. Levi, M.D. Levi, G. Salitra, D. Aurbach, R. Oesten, U. Heider, L. Heider, Solid State Ionics 126 (1999) 97.